Supplementary Information for

Development of an offline Aerosol Mass Spectrometry methodology for organic aerosol characterization in a globally distributed Surface Particulate Matter Network

Yuxuan Ren et al.

Correspondence to: Lu Xu (xu1@wustl.edu) and Randall V. Martin (rvmartin@wustl.edu)

Contents of this file

This Supplementary Information contains Text S1 to Text S4, Table S1 and Table S2, and Figures S1 to S10.

Text S1. Nebulization Efficiency

Nebulization efficiency (NE) is defined as the ratio of AMS-measured mass to the mass of solute nebulized for each component. We quantify NE by nebulizing 2 mL of binary solutions containing varying proportions of sulfate and organic species at a fixed total solute concentration of 40 mg/L. The organic species examined include glucose, DL-4-hydroxy-3-methoxymandelic acid (HMMA), and poly(ethylene glycol) (PEG-400). Figure S3 shows the relationship between solution mass and NE for sulfate and the organic species. NE ranges from 0.70–1.1 % for glucose, 0.43–1.0 % for HMMA, and 1.5–3.8 % for PEG-400, while sulfate NE ranges from 0.23–1.3 %. Differences in NE among the organic species are likely associated with variations in their relative ionization efficiency (RIE). For a given organic species at a fixed total solute concentration in binary solutions, NE varies with the organic-to-sulfate ratio. The highest NE for both organic and sulfate components occurs at an organic-to-sulfate ratio of 0.28 for glucose and HMMA, and 2.0 for PEG-400. This behavior may reflect AMS matrix effects, however, confirming this would require additional laboratory investigation beyond the scope of this study using the standard AMS vaporizer (Xu et al., 2018).

Text S2. Error Propagation

Uncertainties in the offline AMS quantification are propagated through each step of the calculation using standard error propagation. Each filter extract generates 8–12 AMS runs using the current nebulization system.

For each filter extract, the uncertainty in the mean AMS concentration for species *i* is calculated as:

$$\sigma_{\bar{I}_{i,AMS}} = \frac{1}{N}\sqrt{\sum_{k=1}^{N}\left(0.2I_{k,i}\right)^2} \quad (1)$$

$$\sigma_{\bar{I}_i} = \sqrt{\sigma_{\bar{I}_{i,AMS}}^2 + \sigma_{\bar{I}_{i,rep}}^2} \quad (2)$$

where $\sigma_{\bar{I}_{i,AMS}}$ represents AMS measurement uncertainty, with a relative measurement uncertainty of 20 % applied to each run *k* for all species following Bahreini et al. (2009) and Middlebrook et al. (2012), and $\sigma_{\bar{I}_{i,rep}}$ is estimated as the standard deviation across *N* runs for species *i* representing reproducibility.

The uncertainty in the blank-corrected mean AMS concentration for species *i* is calculated as:

$$\sigma_{\Delta I_i} = \sqrt{\sigma_{\bar{I}_i}^2 + \sigma_{\bar{I}_{i,LB}}^2} \quad (3)$$

where $\sigma_{\bar{I}_{i,LB}}$ is the uncertainty in the corresponding mean laboratory blank (LB) concentration for species *i*, calculated using the same approach as for the sample runs.

The uncertainty in organic-to-sulfate ratio measured by AMS for each extract is calculated as:

$$\sigma_{\phi_{AMS}} = \phi_{AMS}\sqrt{\left(\frac{\sigma_{\Delta I_{OA}}}{\Delta I_{OA}}\right)^2 + \left(\frac{\sigma_{\Delta I_{sulfate}}}{\Delta I_{sulfate}}\right)^2} \quad (4)$$

where $\phi_{AMS} = \Delta I_{OA}/\Delta I_{sulfate}$ is the organic-to-sulfate ratio for the filter extract.

The uncertainty in the calibrated organic-to-sulfate ratio in the extract, $\sigma_{\phi_{extract}}$, is estimated by combining the propagated uncertainty from ϕ_{AMS} and uncertainty associated with calibration curve:

$$\sigma_{\phi_{extract}} = \sqrt{\sigma^2_{\phi_{extract,AMS}} + \sigma^2_{extract,cal}} = \sqrt{\left(f'(\phi_{AMS})\sigma_{\phi_{AMS}}\right)^2 + (0.2\phi_{extract})^2} \quad (5)$$

where $f'(\phi_{AMS}) = \frac{1}{\sqrt{1.9912+0.24\phi_{AMS}}}$ is the derivative of the inverse calibration function evaluated at ϕ_{AMS}. The inverse calibration function is $\phi_{extract} = \frac{-1.4+\sqrt{1.9912+0.24\phi_{AMS}}}{0.12}$, corresponding to the calibration relationship $\phi_{AMS} = 0.060\phi^2_{extract} + 1.4\phi_{extract} - 0.13$. The calibration uncertainty $\sigma_{\phi_{extract,cal}}$ is represented as a 20 % relative uncertainty (Section 3.2) and scaled to $\phi_{extract}$.

Finally, the relative uncertainty in the offline OA concentration is calculated as:

$$\frac{\sigma_{C_{OA,offline}}}{C_{OA,offline}} = \sqrt{\left(\frac{\sigma_{\phi_{extract}}}{\phi_{extract}}\right)^2 + \left(\frac{\sigma_{C_{sulfate,extract}}}{C_{sulfate,extract}}\right)^2 + \left(\frac{\sigma_{V_{extract}}}{V_{extract}}\right)^2 + \left(\frac{\sigma_{V_{air}}}{V_{air}}\right)^2} \quad (6)$$

where $\frac{\sigma_{C_{sulfate,extract}}}{C_{sulfate,extract}}$ represents the relative uncertainty in sulfate concentration in the extract, estimated from the analytical precision of Ion Chromatography (IC) sulfate measurements (2.5 %). The relative uncertainty in extract volume, $\frac{\sigma_{V_{extract}}}{V_{extract}}$, is estimated from syringe dispensing precision (2.7 %). The relative uncertainty in sampled air volume, $\frac{\sigma_{V_{air}}}{V_{air}}$, is estimated as the relative standard deviation from 120 flow rate measurements of six flow meters (3.5 %) (Liu et al., 2024).

Text S3. Statistics Calculation

We use the ordinary least-squares or reduced major axis fit (*y*), coefficient of determination (r^2), normalized mean bias (NMB), and normalized root mean square difference (NRMSD) to

evaluate concentrations derived from the offline AMS methodology ($C_{offline}$) against co-located online AMS measurements (C_{online}) across a total of N samples.

$$NMB = \frac{\sum_{i=1}^{N}(C_{offline,i} - C_{online,i})}{\sum_{i=1}^{N} C_{online,i}} \quad (7)$$

$$NRMSD = \frac{\sqrt{\sum_{i=1}^{N}(C_{offline,i} - C_{online,i})^2}}{\sum_{i=1}^{N} C_{online,i}} \quad (8)$$

where $C_{offline,i}$ is the OA concentration determined using the offline AMS methodology for filter sample i, and $C_{online,i}$ is the corresponding OA concentration from online AMS measurements averaged over the filter sampling period.

We perform weighted non-negative least squares (NNLS) regression to quantify factor contributions to offline AMS measurements.

At each time step t, the offline AMS OA mass spectra is represented as a linear combination of fixed factor profiles derived from online positive matrix factorization (PMF) analysis:

$$\mathbf{y}_t \approx \mathbf{F}\boldsymbol{\beta}(t) \quad (9)$$

where $\mathbf{y}_t$ is the offline OA spectra, $\mathbf{F}$ is the online-derived factor profiles, and $\boldsymbol{\beta}(t)$ is the time-dependent factor contributions, constrained to be non-negative.

To account for measurement uncertainty, regression is performed using uncertainty-weighted NNLS:

$$\min_{\beta(t)\geq 0} \sum_{j=1}^{M} \left(\frac{y_{t,j} - \sum_{k=1}^{K} F_{t,j}\beta_k(t)}{\sigma_{t,j}} \right)^2 \quad (10)$$

where $\sigma_{t,j}$ is the uncertainty of the offline signal at m/z bin j.

The weighted problem is then converted by scaling observations and factor profiles by their uncertainties:

$$y'_{t,j} = \frac{y_{t,j}}{\sigma_{t,j}}, F'_{t,j} = \frac{F_{t,j}}{\sigma_{t,j}} \quad (11)$$

yielding:

$$\min_{\beta(t)\geq 0} \|\mathbf{y}'_t - \mathbf{F}'\boldsymbol{\beta}(t)\|_2^2 \quad (12)$$

Text S4. Inorganic Ion Evaluation and Sampling Effects

We conduct a pilot study to evaluate offline AMS measurements with co-located online AMS measurements and complementary offline measurements. In addition to OA and sulfate discussed in Section 3.3.2, ammonium and nitrate are further evaluated here. Offline AMS ammonium and nitrate are quantified using sulfate as the internal standard, following the same

approach as for OA, with the assumption of a unity calibration slope between ammonium-to-sulfate and nitrate-to-sulfate ratios in the extract and in the AMS. Ammonium determined by the offline AMS method shows strong agreement with IC measurements, with a slope of 1.1 and r^2 of 0.93 (Figure S8d), supporting the reliability of the offline quantification. In contrast, we find poor agreement between offline and online AMS for both ammonium and nitrate (Figure S8c and Figure S8e), likely reflecting measurement uncertainties, volatilization losses, and interferences associated with filter-based sampling and extraction. To enable a more direct comparison with IC measurements of inorganic nitrate, total nitrate from offline AMS is further partitioned using the NO^+/NO_2^+ ratio method (Day et al., 2002; Farmer et al., 2010; Xu et al., 2015). In this approach, the NO^+/NO_2^+ ratio for ammonium nitrate is 1.8 ± 0.16 based on instrument-specific ionization efficiency calibration, while the ratio for organic nitrates is assumed to be 2.25 (range 2.08–3.99) times higher than that of ammonium nitrate. Based on this approach, inorganic nitrate accounts for 52 ± 19 % of total offline AMS nitrate (mean ± standard deviation), with a median of 49 % (39 % and 68 % for the first and third quartiles, respectively). Despite this correction, offline AMS-derived nitrate remains systematically higher than IC nitrate (Figure S8f), likely reflecting uncertainties in the inorganic nitrate apportionment and the low IC nitrate concentrations approaching detection limits.

Differences in sampled particle size do not substantially affect online-offline agreement, as filters corresponding to $PM_{2.5}$ and PM_1 cut sizes yield comparable OA recoveries (Figure S10). This observation is consistent with prior findings that 91 % of sulfate and 86 % of organic carbon $PM_{2.5}$ mass are within the PM_1 size range (Li et al., 2025). Evaporation losses of volatile and semi-volatile species during filter collection may also contribute to differences between online and offline measurements. However, such losses are generally recognized as an inherent limitation of filter-based sampling approaches and are therefore not quantified here (Srivastava et al., 2021).

Supplementary Tables

Table S1. Analyte concentrations for each solution in calibration curves. Solutions are prepared from stock solutions of ammonium sulfate (AS), glucose, DL-4-hydroxy-3-methoxymandelic acid (HMMA), and poly(ethylene glycol) (PEG-400).

Sample	Organics	AS Volume (mL)	Organic Volume (mL)	Ultrapure Water Volume (mL)	Total Volume (mL)	Total Concentration (mg/L)	AS Concentration (mg/L)	Organic Concentration (mg/L)	Solution Organic-to-sulfate Ratio
G1	Glucose	0.1	1	1.65	2.75	40	3.6	36.4	14
G2	Glucose	0.2	1	1.8	3	40	6.7	33.3	6.9
G3	Glucose	0.5	1	2.25	3.75	40	13.3	26.7	2.8
G4	Glucose	0.7	1	2.55	4.25	40	16.5	23.5	2.0
G5	Glucose	1	1	3	5	40	20.0	20.0	1.4
G6	Glucose	1	0.7	2.55	4.25	40	23.5	16.5	1.0
G7	Glucose	1	0.5	2.25	3.75	40	26.7	13.3	0.69
G8	Glucose	1	0.2	1.8	3	40	33.3	6.7	0.28
G9	Glucose	1.5	0.2	2.55	4.25	40	35.3	4.7	0.18
H1	HMMA	0.1	1	1.65	2.75	40	3.6	36.4	13.8
H2	HMMA	0.2	1	1.8	3	40	6.7	33.3	6.9
H3	HMMA	0.5	1	2.25	3.75	40	13.3	26.7	2.8
H4	HMMA	0.7	1	2.55	4.25	40	16.5	23.5	2.0
H5	HMMA	1	1	3	5	40	20.0	20.0	1.4
H6	HMMA	1	0.7	2.55	4.25	40	23.5	16.5	1.0
H7	HMMA	1	0.5	2.25	3.75	40	26.7	13.3	0.69
H8	HMMA	1	0.2	1.8	3	40	33.3	6.7	0.28
H9	HMMA	1.5	0.2	2.55	4.25	40	35.3	4.7	0.18
P1	PEG-400	0.1	1	1.65	2.75	40	3.6	36.4	14
P2	PEG-400	0.2	1	1.8	3	40	6.7	33.3	6.9
P3	PEG-400	0.5	1	2.25	3.75	40	13.3	26.7	2.8
P4	PEG-400	0.7	1	2.55	4.25	40	16.5	23.5	2.0
P5	PEG-400	1	1	3	5	40	20.0	20.0	1.4
P6	PEG-400	1	0.7	2.55	4.25	40	23.5	16.5	1.0
P7	PEG-400	1	0.5	2.25	3.75	40	26.7	13.3	0.69
P8	PEG-400	1	0.2	1.8	3	40	33.3	6.7	0.28
P9	PEG-400	1.5	0.2	2.55	4.25	40	35.3	4.7	0.18

Table S2. Method detection limits (MDLs) of OA, sulfate, nitrate, ammonium, and chloride. Online detection limits are determined from filtered air analyses. Offline detection limits are calculated from ultrapure water blanks, field blanks, and laboratory blanks. *N* represents the number of AMS runs included in each calculation.

		N	OA	Sulfate	Nitrate	Ammonium	Chloride
Online ($\mu g/m^3$)	Filtered air	357	0.17	0.031	0.015	0.0020	0.031
Offline ($\mu g/m^3$)*	Ultrapure water	65	1.5	1.2	1.5	0.33	0.085
	Field blank	64	7.1	1.1	2.3	0.086	0.72
	Laboratory blank	62	5.5	0.57	2.1	0.49	0.30

* Offline MDLs are reported here in units of $\mu g/m^3$. To convert to mass on filter (μg), the median nebulization efficiency for each species is applied to convert the mass measured by the offline AMS to the corresponding mass in solution.

Supplementary Figures

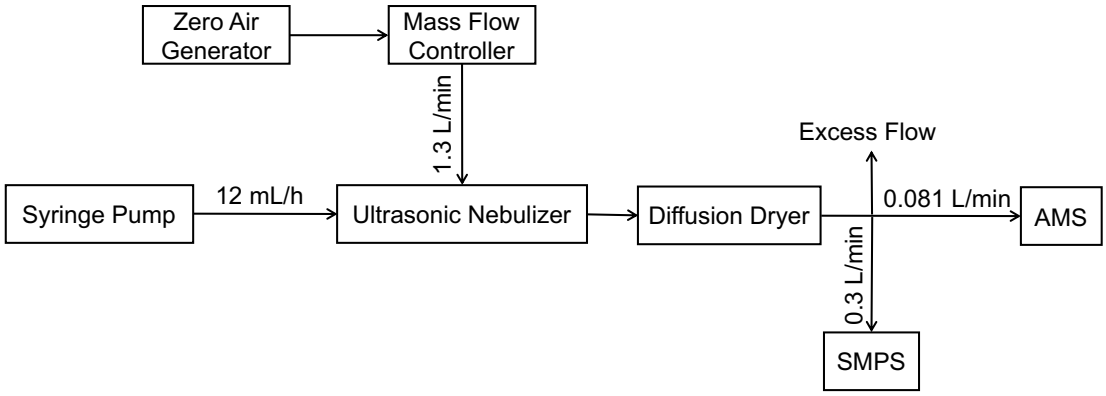

Figure S1. Simplified schematic of the setup for offline AMS methodology.

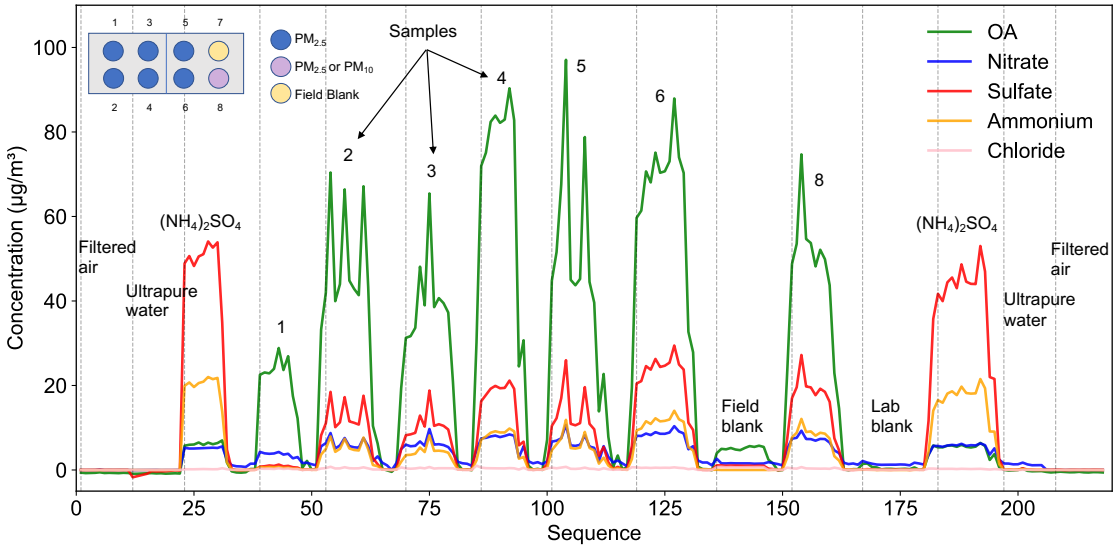

Figure S2. Representative AMS measurement cycle showing raw data for OA (green), nitrate (blue), sulfate (red), ammonium (orange), and chloride (pink). Periods corresponding to filtered air, ultrapure water, ammonium sulfate ($(NH_4)_2SO_4$) solution, filter samples, field blanks, and laboratory blanks are indicated. The top-left panel illustrates the SPARTAN cartridge configuration, in which eight filters are assembled for site deployment, with filters 1 to 6 for $PM_{2.5}$ samples, filter 8 for either a $PM_{2.5}$ or PM_{10} sample depending on the protocol, and filter 7 left unexposed to airflow to serve as a field blank.

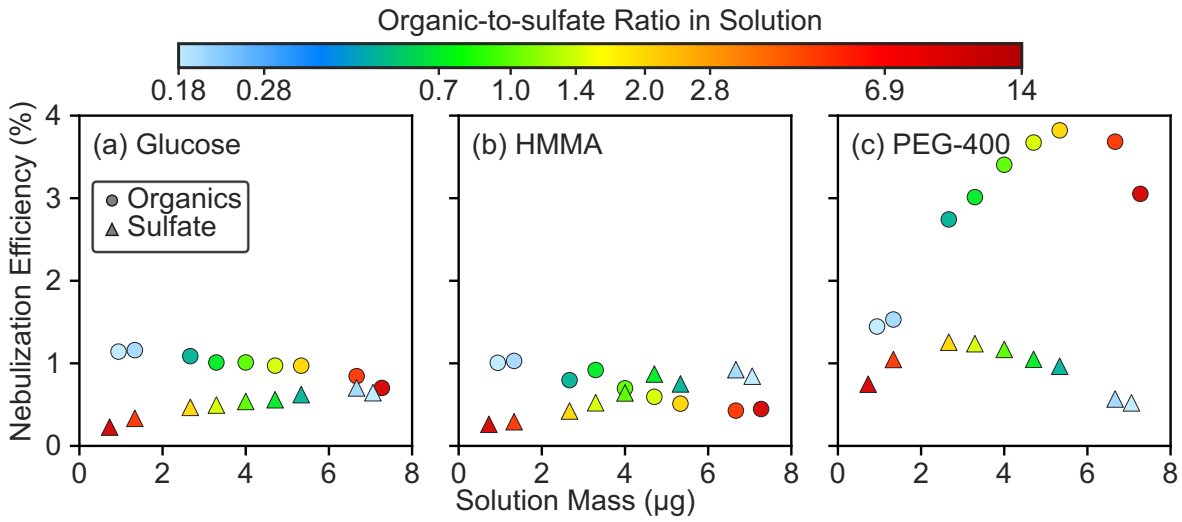

Figure S3. Solution mass loaded into the syringe compared to nebulization efficiency for sulfate and organic components in binary solutions containing (a) glucose, (b) DL-4-Hydroxy-3-methoxymandelic acid (HMMA), and (c) poly(ethylene glycol) (PEG-400). Organic components are combined with sulfate across nine concentration levels, each prepared at a fixed total solute concentration of 40 mg/L. Points are colored by the organic-to-sulfate ratio in solution, with circles representing organic components and triangles representing sulfate. Nebulization efficiency is defined as the ratio of AMS-measured mass to the mass of solute nebulized for each component.

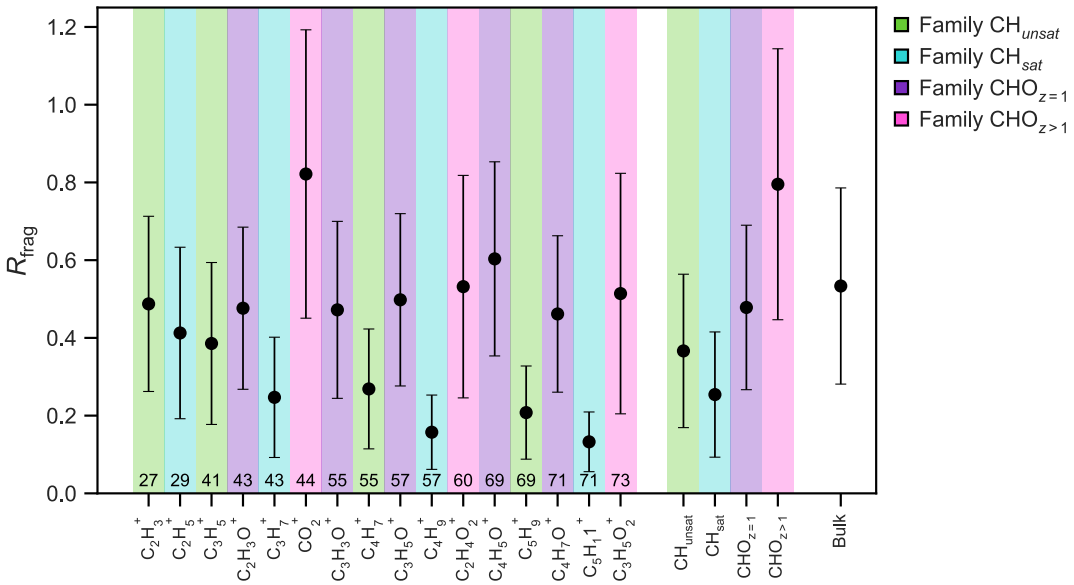

147

148 Figure S4. Recovery (mean ± standard deviation) of individual organic fragments and chemical
149 families for samples collected in St. Louis. Recovery (R_{frag}) is calculated as the ratio of offline
150 concentrations to the corresponding online measurements, with a value of 1 indicating 100 %
151 recovery. Fragments are color-coded by family, including mono-oxygenated ions ($CHO_{z=1}$),
152 poly-oxygenated ions ($CHO_{z>1}$), saturated hydrocarbons (CH_{sat}), and unsaturated hydrocarbons
153 (CH_{unsat}). Numbers inserted indicate the nominal mass of each fragment. Families include all
154 respective fragments weighted by their mass contribution.

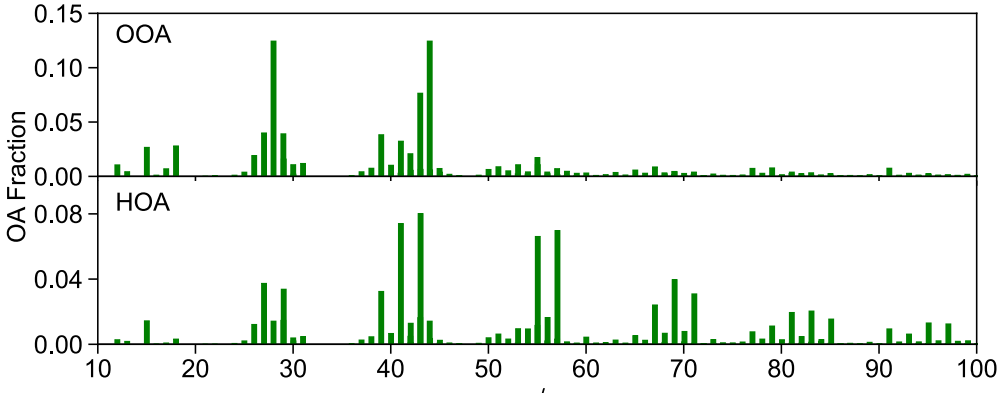

155

156 Figure S5. Factor profiles from the selected positive matrix factorization (PMF) solution
157 applied to online AMS measurements in St. Louis, resolving oxygenated OA (OOA) and
158 hydrocarbon-like OA (HOA).

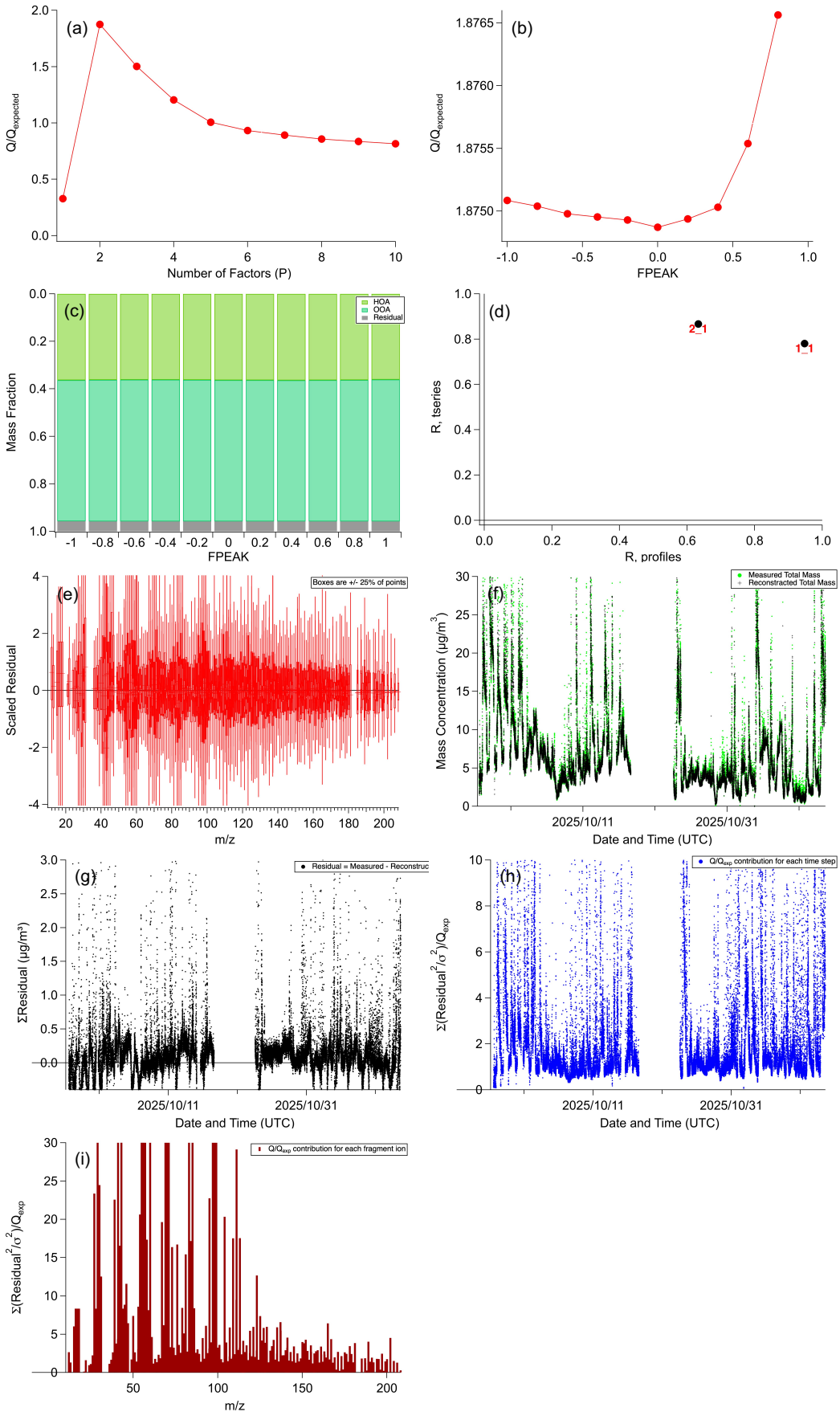
(a)
Q/Q_expected
Number of Factors (P)
(b)
Q/Q_expected
FPEAK
(c)
HOA
OOA
Residual
Mass Fraction
FPEAK
(d)
2_1
1_1
R, tseries
R, profiles
(e)
Boxes are +/- 25% of points
Scaled Residual
m/z
(f)
Measured Total Mass
Reconstructed Total Mass
Mass Concentration (µg/m3)
2025/10/11
2025/10/31
Date and Time (UTC)
(g)
Residual = Measured - Reconstruc
ΣResidual (µg/m³)
2025/10/11
2025/10/31
Date and Time (UTC)
(h)
Q/Q_exp contribution for each time step
Σ(Residual²/σ²)/Q_exp
2025/10/11
2025/10/31
Date and Time (UTC)
(i)
Q/Q_exp contribution for each fragment ion
Σ(Residual²/σ²)/Q_exp
m/z

159

Figure S6. Summary of key diagnostic plots of the positive matrix factorization (PMF) analysis of online samples collected in St. Louis. (a) Q/Q_{exp} as a function of the number of factors; (b) Q/Q_{exp} as a function of FPEAK for the 2-factor solution; (c) mass fraction of PMF factors as a function of FPEAK; (d) correlations of time series and mass spectra among PMF factors; (e) distribution of scaled residuals for each m/z, where boxes represent the interquartile range (25th–75th percentile); (f) time series of measured and reconstructed organic mass; (g) residual of the least-square fit as a function of time; (h) Q/Q_{exp} for each data point as a function of time, and (i) Q/Q_{exp} values for each m/z.

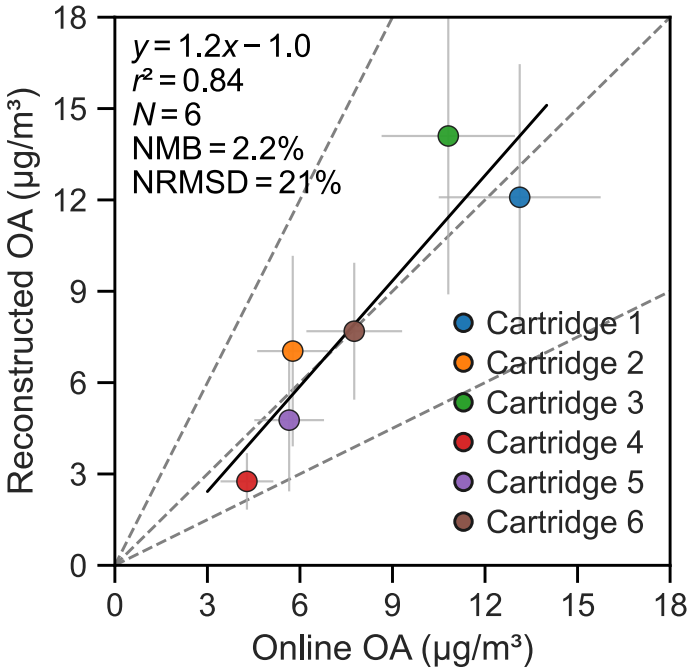

Figure S7. Comparison of reconstructed OA concentrations with online OA concentrations for cartridges collected in St. Louis. Reconstructed OA concentrations are calculated by dividing each offline-derived factor by its mean recovery. Horizontal bars indicate the estimated AMS measurement uncertainty of online OA concentrations, while vertical bars indicate the propagated uncertainty of offline OA concentrations. Data are shown as cartridge-level means and are colored by cartridge. Annotations indicate the ordinary least-squares fit (y), coefficient of determination (r^2), number of comparison points (N), Normalized Mean Bias (NMB), and Normalized Root Mean Square Deviation (NRMSD). Dashed lines indicate reference lines with slopes of 0.5, 1, and 2.

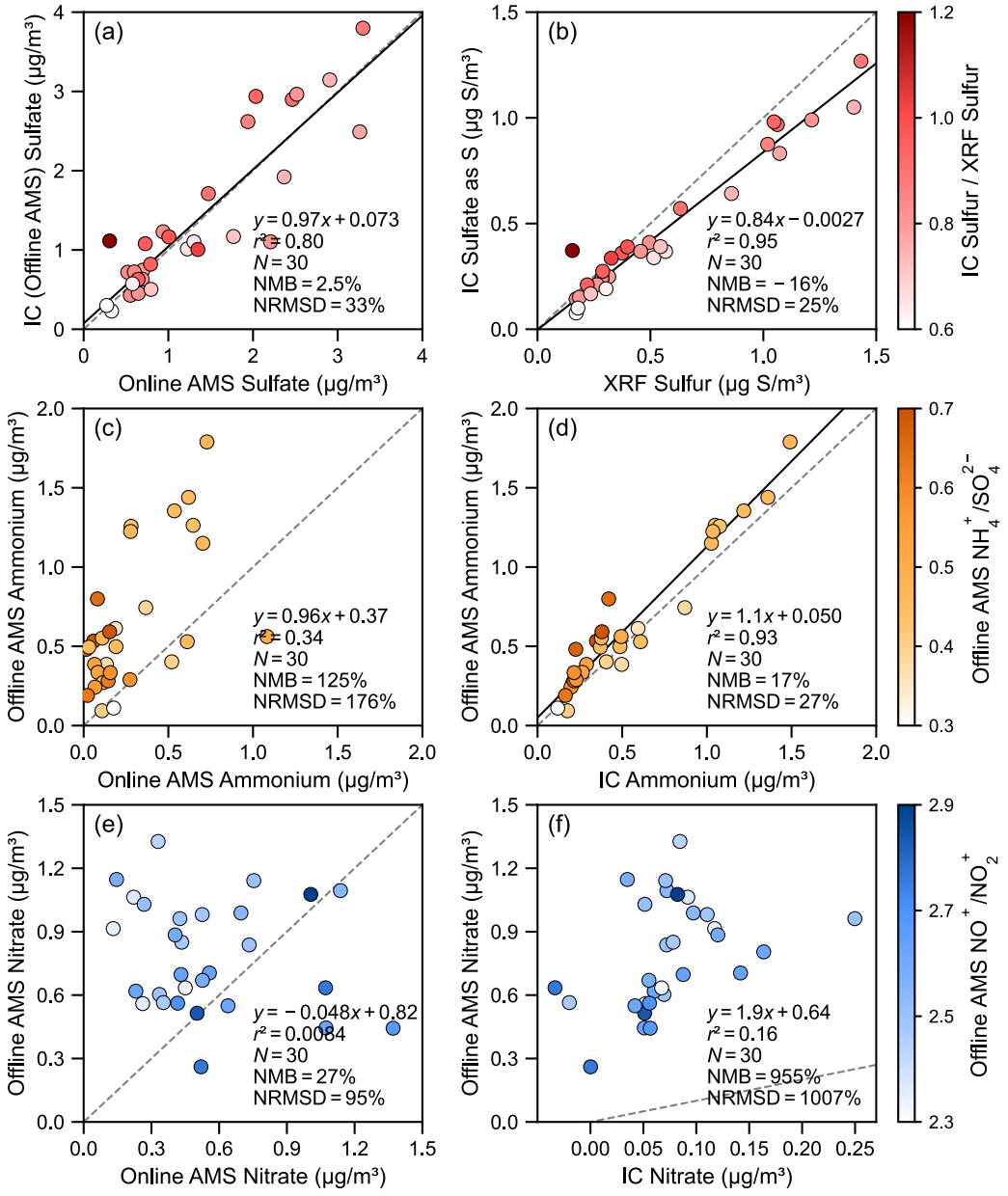

178

179 Figure S8. Comparison of sulfate, ammonium, and nitrate concentrations derived from offline
180 AMS with co-located online AMS and complementary offline measurements for samples
181 collected in St. Louis. Panels (a), (c), and (e) compare offline AMS with online AMS for sulfate,
182 ammonium, and nitrate, respectively, panel (b) compares offline AMS sulfate (expressed as S)
183 with sulfur measured by X-ray fluorescence (XRF), and panels (d) and (f) compare offline
184 AMS ammonium and nitrate with concentrations measured by Ion Chromatography (IC).
185 Offline AMS sulfate is intrinsically linked to IC sulfate through its use as the internal standard
186 and is therefore treated equivalently in this comparison. Offline AMS ammonium and nitrate
187 are quantified using sulfate as the internal standard, assuming a unity calibration slope. Online
188 AMS concentrations represent time-averaged values over each corresponding filter sampling

interval, while offline AMS concentrations represent the mean across 8 to 12 runs. Data points are colored by IC sulfur to XRF sulfur ratio in red for (a) and (b), offline AMS ammonium-to-sulfate ratio in orange for (c) and (d), and offline AMS NO^+/NO_2^+ ratio in blue for (e) and (f). Annotations indicate the reduced major axis fit (*y*) for (b) and the ordinary least-squares fit (*y*) for the remaining panels, coefficient of determination (r^2), number of comparison points (*N*), Normalized Mean Bias (NMB), and Normalized Root Mean Square Deviation (NRMSD). The dashed line indicates the 1:1 reference.

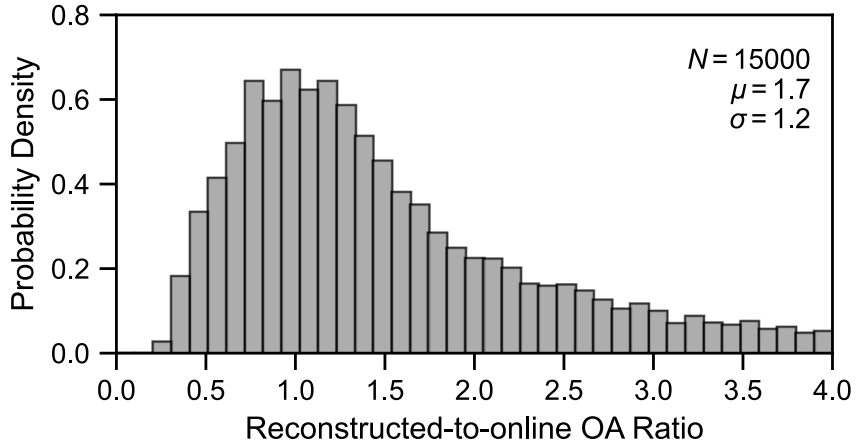

Figure S9. Histogram of reconstructed-to-online OA concentration ratios for samples collected in St. Louis. Reconstructed OA is obtained by separating offline OA into oxygenated OA (OOA) and hydrocarbon-like OA (HOA) using weighted non-negative least-squares (NNLS) regression, and extrapolating each factor by its corresponding recovery. The regression uses factor profiles derived from this study (online AMS) and four additional OOA and HOA profile pairs from the AMS Spectral Database. OOA and HOA recoveries are sampled 100 times from representative ranges (0.36–0.92 for OOA and 0.028–0.17 for HOA) based on this and previous offline AMS studies. Calculations are performed for 30 samples using five factor-profile combinations and 100 bootstrap realizations per combination. Online OA represents the time-averaged concentration over each corresponding filter sampling interval. Annotations indicate the number of points (*N*), and the mean (μ) and standard deviation (σ) of the fitted normal distribution.

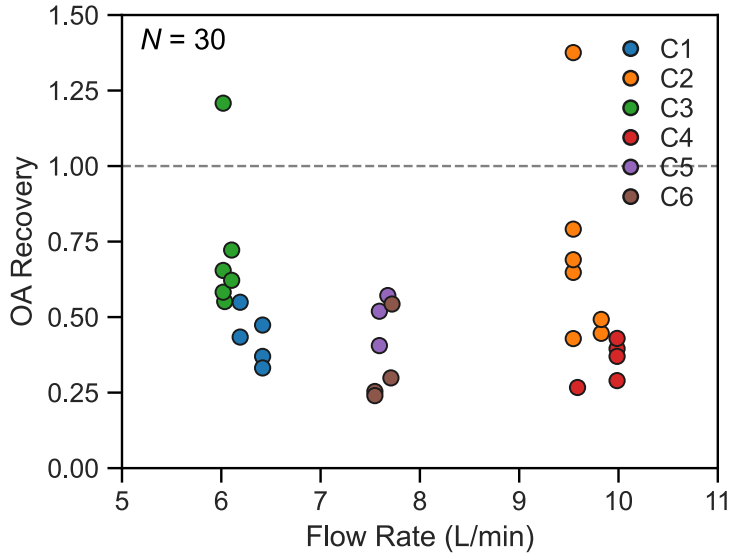

Figure S10. OA recovery compared to the flow rate upstream of the PM cyclone. A flow rate of 5 L/min corresponds to a cut size of $PM_{2.5}$, while 11 L/min corresponds to a PM_1 cut size. Data are shown for individual filters collected in St. Louis and are colored by cartridge (C1–C6).

References

Bahreini, R., Ervens, B., Middlebrook, A.M., Warneke, C., de Gouw, J.A., DeCarlo, P.F., Jimenez, J.L., Brock, C.A., Neuman, J.A., Ryerson, T.B., Stark, H., Atlas, E., Brioude, J., Fried, A., Holloway, J.S., Peischl, J., Richter, D., Walega, J., Weibring, P., Wollny, A.G., and Fehsenfeld, F.C.: Organic aerosol formation in urban and industrial plumes near Houston and Dallas, Texas, J. Geophys. Res.-Atmos., 114, D00F16, 2009.

Day, D.A., Wooldridge, P.J., Dillon, M.B., Thornton, J.A., and Cohen, R.C.: A thermal dissociation laser-induced fluorescence instrument for in situ detection of NO_2, peroxy nitrates, alkyl nitrates, and HNO_3, J. Geophys. Res.-Atmos., 107, ACH 4-1–ACH 4-14, 2002.

Farmer, D.K., Matsunaga, A., Docherty, K.S., Surratt, J.D., Seinfeld, J.H., Ziemann, P.J., and Jimenez, J.L.: Response of an aerosol mass spectrometer to organonitrates and organosulfates and implications for atmospheric chemistry, Proc. Natl. Acad. Sci. USA, 107, 6670–6675, 2010.

Li, C., Martin, R.V., van Donkelaar, A., Jimenez, J.L., Zhang, Q., Turner, J.R., Liu, X., Rowe, M., Meng, J., Yu, W., and Thurston, G.D.: Estimates of submicron particulate matter (PM_1) concentrations for 1998–2022 across the contiguous USA: Leveraging measurements of PM_1 with nationwide $PM_{2.5}$ component data, Lancet Planet. Health, 9, e491–e502, 2025.

Liu, X., Turner, J.R., Oxford, C.R., McNeill, J., Walsh, B., Le Roy, E., Weagle, C.L., Stone, E., Zhu, H., Liu, W., Wei, Z., Hyslop, N.P., Giacomo, J., Dillner, A.M., Salam, A., Hossen, A.-A., Islam, Z., Abboud, I., Akoshile, C., Amador-Munoz, O., Anh, N.X., Asfaw, A., Balasubramanian, R., Chang, R.Y.W., Coburn, C., Dey, S., Diner, D.J., Dong, J., Farrah, T., Gahungu, P., Garland, R.M., Grutter de la Mora, M., Hasheminassab, S., John, J., Kim, J., Kim, J.S., Langerman, K., Lee, P.C., Lestari, P., Liu, Y., Mamo, T., Martins, M., Mayol-Bracero, O.L., Naidoo, M., Park, S.S., Schechner, Y., Schofield, R., Tripathi, S.N., Windwer, E., Wu, M.T., Zhang, Q., Brauer, M., Rudich, Y., and Martin, R.V.: Elemental characterization of ambient particulate matter for a globally distributed monitoring network: Methodology and implications, Environ. Sci. Technol. Air, 1, 283–293, 2024.

Middlebrook, A.M., Bahreini, R., Jimenez, J.L., and Canagaratna, M.R.: Evaluation of composition-dependent collection efficiencies for the aerodyne aerosol mass spectrometer using field data, Aerosol Sci. Technol., 46, 258–271, 2012.

Srivastava, D., Daellenbach, K.R., Zhang, Y., Bonnaire, N., Chazeau, B., Perraudin, E., Gros, V., Lucarelli, F., Villenave, E., Prevot, A.S.H., El Haddad, I., Favez, O., and Albinet, A.:

Comparison of five methodologies to apportion organic aerosol sources during a PM pollution event, Sci. Total Environ., 757, 143168, 2021.

Xu, L., Suresh, S., Guo, H., Weber, R.J., and Ng, N.L.: Aerosol characterization over the southeastern United States using high-resolution aerosol mass spectrometry: Spatial and seasonal variation of aerosol composition and sources with a focus on organic nitrates, Atmos. Chem. Phys., 15, 7307–7336, 2015.

Xu, W., Lambe, A., Silva, P., Hu, W., Onasch, T., Williams, L., Croteau, P., Zhang, X., Renbaum-Wolff, L., Fortner, E., Jimenez, J.L., Jayne, J., Worsnop, D., and Canagaratna, M.: Laboratory evaluation of species-dependent relative ionization efficiencies in the aerodyne aerosol mass spectrometer, Aerosol Sci. Technol., 52, 626–641, 2018.